ELSEVIER

SCIENCE DIRECT®

PHYSICS LETTERS B

Physics Letters B 578 (2004) 63–68

www.elsevier.com/locate/physletb

Double π^0 photoproduction off the proton at threshold

M. Kotulla [a], J. Ahrens [b], J.R.M. Annand [c], R. Beck [b], D. Hornidge [b], S. Janssen [d], B. Krusche [a], J.C. McGeorge [c], I.J.D. MacGregor [c], J.G. Messchendorp [e], V. Metag [d], R. Novotny [d], M. Pfeiffer [d], R.O. Owens [c], M. Rost [b], S. Schadmand [d], D.P. Watts [c]

[a] *Department of Physics and Astronomy, University of Basel, CH-4056 Basel, Switzerland*
[b] *Institut für Kernphysik, Johannes-Gutenberg-Universität Mainz, D-55099 Mainz, Germany*
[c] *Department of Physics and Astronomy, University of Glasgow, Glasgow G12 8QQ, UK*
[d] *II. Physikalisches Institut, Universität Gießen, D-35392 Gießen, Germany*
[e] *KVI, Zernikelaan 25, 9747 AA Groningen, The Netherlands*

Received 16 September 2003; received in revised form 9 October 2003; accepted 15 October 2003

Editor: J.P. Schiffer

Abstract

The reaction $\gamma p \to \pi^0\pi^0 p$ has been measured using the TAPS BaF_2 calorimeter at the tagged photon facility of the Mainz Microtron accelerator. Chiral perturbation theory (ChPT) predicts that close to threshold this channel is significantly enhanced compared to double pion final states with charged pions. In contrast to other reaction channels, the lower order tree terms are strongly suppressed in $2\pi^0$ photoproduction. The consequence is the dominance of pion loops in the $2\pi^0$ channel close to threshold—a result that opens new prospects for the test of ChPT and in particular its inherent loop terms. The present measurement is the first which is sensitive enough for a conclusive comparison with the ChPT calculation and is in agreement with its prediction. The data also show good agreement with a calculation in the unitary chiral approach.

PACS: 11.30.Rd; 13.60.Le; 25.20.Lj

1. Introduction

In the energy regime where excitations of the nucleon or properties of the lowest lying mesons are studied, the perturbative ansatz to solve QCD fails, because the strong coupling constant α_s is too large. A different approach exploiting the approximate Goldstone boson nature of the pion has been developed, namely chiral perturbation theory (ChPT) [12,23]. This effective field theory has been extended to the nucleon sector (HBChPT[1]) [5,15]. Historically, it was a great success that ChPT could clarify the disagreement between the old low-energy theorems (LETs) in describing the s-wave threshold amplitude E_{0+} in the reaction $\gamma p \to \pi^0 p$ [3,18]. Additional contributions due to pion loops had to

E-mail address: martin.kotulla@unibas.ch (M. Kotulla).

[1] ChPT is used in this Letter as a synonym for HBChPT

0370-2693
doi:10.1016/j.physletb.2003.10.056

be added to the old LETs, resulting in a lower value for the E_{0+} amplitude and agreement with measured data [4]. In general, ChPT is in good agreement with experiments describing π–N scattering [10].

From the study of $\pi\pi$ production processes, complementary information to the study of the single pion photoproduction channels can be gained. The extention of ChPT to $\pi\pi$ photo- and electroproduction has led to the finding that the cross section for final states with two neutral pions is dramatically enhanced due to chiral (pion) loops [6] which appear in leading (non-vanishing) order q^3. This is a counter-intuitive result, since in the case of single pion production the cross sections for charged pions are considerably larger than those with neutral pions in the final state. This situation is not changed when the ChPT calculation is extended by evaluating all next-to-leading order terms up to order M_π^2 in the threshold amplitude [8]. Exploring this situation in more detail, the two pion channel exhibits the following properties [8]: Born type contributions start at order M_π and are very small. Tree diagrams up to order q^3 are zero due to threshold selection rules or pairwise cancellation. Only at order q^4 do tree terms proportional to the low energy constants c_i give a moderate contribution. In a microscopic picture these tree terms ($\propto c_i$) subsume all s-, t- and u-channel resonances in the $\pi^0 p$ scattering amplitude (e.g., the $\Delta(1232)$). The largest resonance contribution at order M_π^2 comes from the $P_{11}(1440)$ resonance via the $N^*N\pi\pi$ s-wave vertex. Possible double Δ graphs as well as loop diagrams containing a photon coupling to a K^+–Σ/Λ pair were estimated and found to be negligible. Fourth order loop diagrams (q^4) provide only a moderate contribution. All the coefficients of the resulting threshold amplitude were taken from the literature, π–N scattering and, in case of the s-wave $P_{11}(1440)$ to $\pi\pi$ coupling, from an analysis of the reaction $\pi N \to \pi\pi N$ [7]. Adding all contributions together, the astonishing result is that the yield of the leading order loop diagrams (q^3) is approximately 2/3 of the total $2\pi^0$ strength. This fact makes this channel unique, because unlike in other channels where the loops are adding some contribution to the dominant tree graphs, here they dominate. Consequently the $2\pi^0$ channel provides a very sensitive method to study these loop contributions to ChPT. In [8], the following prediction for the near threshold cross section was given

$$\sigma_{\text{tot}}(E_\gamma) = (0.6\text{ nb})\left(\frac{E_\gamma - E_\gamma^{\text{thr}}}{10\text{ MeV}}\right)^2, \tag{1}$$

where E_γ denotes the photon beam energy and E_γ^{thr} is the production threshold of 308.8 MeV. Actually, the uncertainty of the coupling of the $P_{11}(1440)$ to the s-wave $\pi\pi$ channel was a limiting factor for the accuracy of the ChPT calculation [8]. For the most extreme case of this coupling, an upper limit for this cross section was deduced by increasing the constant in Eq. (1) from 0.6 to 0.9 nb.

To complete the overview of theoretical calculations of the reaction $\gamma p \to \pi^0\pi^0 p$ close to threshold, it is noted that this channel is also described in a recent version of the Gomez Tejedor–Oset model [21]. This model is based on a set of tree level diagrams including pions, nucleons and nucleonic resonances. In a recent work, particular emphasis was put on the rescattering of pions in the isospin $I = 0$ channel [20]. Double pion photoproduction via the Δ Kroll–Rudermann term is not possible for the $2\pi^0$ final state. In the case of a $\pi^-\pi^+$ Kroll–Rudermann term, the charged pions can rescatter into two neutral pions generating dynamically a $\pi\pi$ loop. This effect nearly doubles the cross section in the threshold region and is regarded by the authors as being reminiscent of the explicit chiral loop effect described above. Nevertheless, the cross section calculated with this model is significantly smaller than the ChPT prediction.

In the past, two measurements of the reaction $\gamma p \to \pi^0\pi^0 p$ below 450 MeV beam energy have been carried out [13,24]. The second experiment showed an improvement in statistics by almost a factor 30. Nevertheless, in the threshold region the cross section still suffered from large statistical uncertainties (see Fig. 2).

In contrast to previous analyses, we did not extract the cross section from events in which only three of the four decay photons were detected. Such analyses are not kinematically overdetermined and, close to threshold in particular, the extracted cross section can be slightly contaminated by the reaction $\gamma p \to \pi^0\gamma p$, which has recently been measured [16]. This present measurement of the $2\pi^0$ photoproduction at threshold is the first for which comparison to theoretical calculations is conclusive.

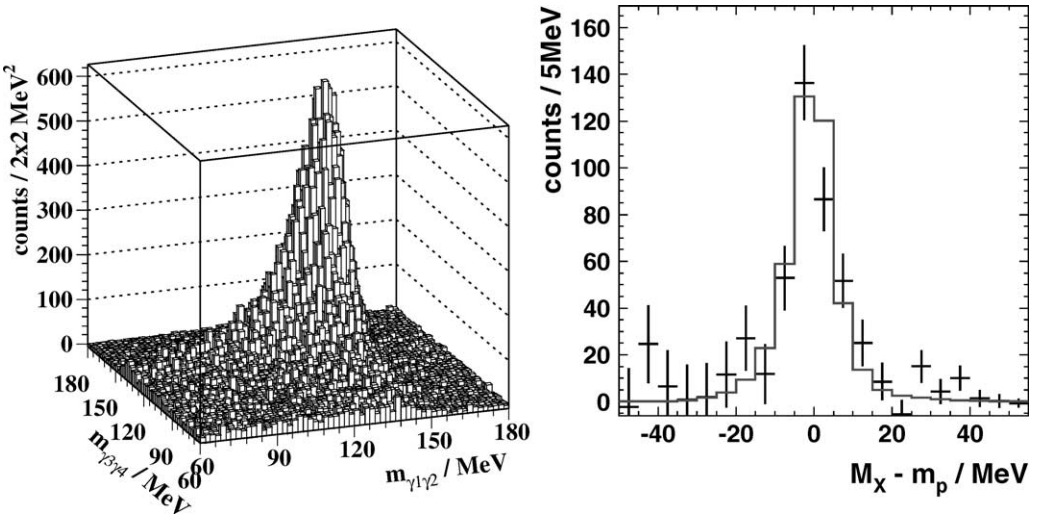

Fig. 1. Left: two photon invariant masses $m_{\gamma 1\gamma 2}$ vs $m_{\gamma 3\gamma 4}$. Right: missing mass $M_X - m_p$ derived from two detected π^0 mesons for incident beam energies $E_\gamma \leqslant 400$ MeV (symbols with errors: data, histogram: GEANT simulation).

2. Experimental setup and data analysis

The reaction $\gamma p \to \pi^0\pi^0 p$ was measured at the Mainz Microtron (MAMI) electron accelerator [1,22] using the Glasgow tagged photon facility [2,14] and the photon spectrometer TAPS [11,19]. A quasi-monochromatic photon beam was produced by bremsstrahlung tagging, in which the photon energy is determined by the difference between the energies of the incident electron and the residual electron following bremsstrahlung because the energy transfer to the atomic nuclei of the radiator foil is negligible. The photon energy covered the range 285–820 MeV with an average energy resolution of 2 MeV. The photon flux was of the order of 0.5 MHz MeV^{-1} at photon energies of 300 MeV. The TAPS detector consisted of six blocks each with 62 hexagonally shaped BaF_2 crystals arranged in an 8×8 matrix and a forward wall with 138 BaF_2 crystals arranged in a 11×14 rectangle. Each crystal is 250 mm long with an inner diameter of 59 mm. The six blocks were located in a horizontal plane around the target at angles of $\pm 54°$, $\pm 103°$ and $\pm 153°$ with respect to the beam axis. Their distance to the target was 55 cm and the distance of the forward wall was 60 cm. This setup covered $\approx 40\%$ of the full solid angle. All BaF_2 modules were equipped with 5 mm thick scintillation plastic dE/dx detectors to allow the identification of charged particles. The liquid hydrogen target was 10 cm long with a diameter of 3 cm. Further details of the experimental setup can be found in Ref. [17].

The $\gamma p \to \pi^0\pi^0 p$ reaction channel was identified by measuring the 4-momenta of the two π^0 mesons, whereas the proton was not detected. For a three-body final state this provides kinematical overdetermination and hence an unambiguous identification of this reaction channel. The π^0 mesons were detected via their two-photon decay channel and identified in a standard invariant mass analysis from the measured photon momenta. The four photons of an event can be arranged in three different combinations to form two 2-photon invariant masses (compare Fig. 1). For an acceptable $(\gamma, \pi^0\pi^0)$ event, one of these combinations was required to fulfill the condition, $110 < m_{\gamma\gamma} < 150$ MeV, for both of the 2-photon invariant masses. In addition the mass of the missing proton was calculated from the beam energy E_{beam}, target mass m_p and the energies E_{π^0} and momenta $\vec{p}_{\pi^0}$ of the pions via

$$M_X^2 = \left((E_{\pi_1^0} + E_{\pi_2^0}) - (E_{\text{beam}} + m_p)\right)^2 - \left((\vec{p}_{\pi_1^0} + \vec{p}_{\pi_2^0}) - (\vec{p}_{\text{beam}})\right)^2. \quad (2)$$

The resulting distribution is shown in Fig. 1. In case of the reaction $\gamma p \to \pi^0\pi^0 p$ the missing mass must be equal to the mass of the (undetected) proton m_p. A Monte Carlo simulation of the $2\pi^0$ reaction using

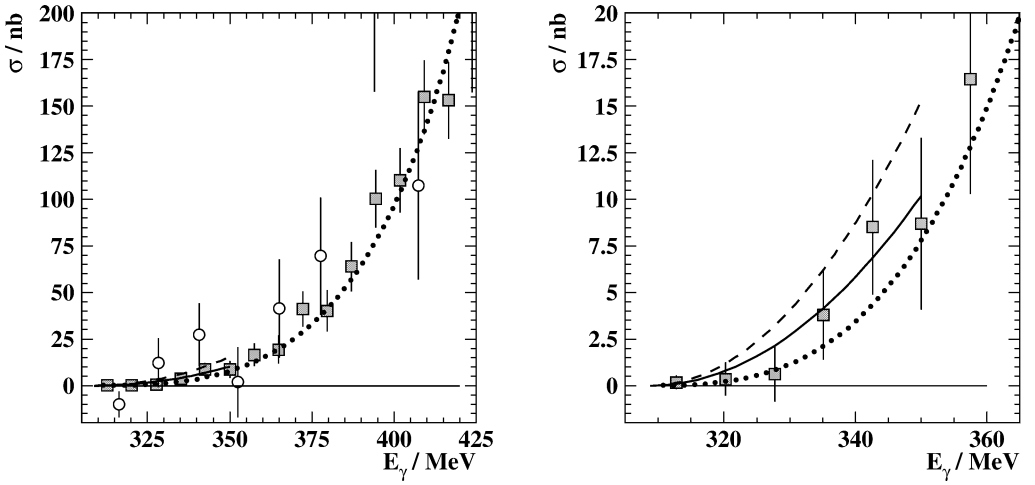

Fig. 2. Total cross section for the reaction $\gamma p \to \pi^0\pi^0 p$ (grey squares) at threshold in comparison with a previous experiment [24] (open circles) for incident energies up to 360 MeV (right) and 425 MeV (left), respectively. The error bars denote the statistical error. The prediction of the ChPT calculation [8] is shown (solid curve) together with its upper limit (dashed curve) and the prediction of Ref. [20] (dotted curve).

GEANT3 [9] reproduces the lineshape of the measured data. A cut corresponding to a $\pm 2\sigma$ width of the simulated lineshape has been applied to select the events of interest. Random time coincidences between the TAPS detector and the tagging spectrometer were subtracted, using events outside the prompt time coincidence window [14]. No systematical errors are introduced by this method and the statistical errors introduced by the subtraction are included in the errors presented in this Letter.

The cross section was deduced from the rate of the $2\pi^0$ events, the number of hydrogen atoms per cm^2, the photon beam flux, the branching ratio of the π^0 decay into two photons, and the detector and analysis efficiency. The intensity of the photon beam was determined by counting the scattered electrons in the tagger focal plane and measuring the loss of photon intensity due to collimation with a 100%-efficient BGO detector which was moved into the photon beam at reduced intensity. The geometrical detector acceptance and analysis efficiency due to cuts and thresholds were obtained using the GEANT3 code and an event generator producing distributions of the final state particles according to phase space. The acceptance of the detector setup was studied by examining independently a grid of the four degrees of freedom for this three body reaction (azimuthal symmetry of the reaction was assumed). In a grid of total 1024 bins no acceptance holes were found for the beam energy range presented in this Letter. The average value for the detection efficiency is 1.0%. The systematic errors are estimated to be 6% and include uncertainties of the beam flux, the target length and the efficiency determination. All results presented in this work are acceptance corrected and absolutely normalized.

3. Results and discussion

The measured total cross section for the reaction $\gamma p \to \pi^0\pi^0 p$ is shown in Fig. 2 as a function of the incident photon beam energy. The results are compared to a previous experiment [24]. The two experiments are consistent within the rather large errors of the previous work.

The prediction of ChPT [8] is plotted up to 40 MeV above the production threshold. The overall shape as well as the absolute magnitude are in agreement with the data. Furthermore, the ChPT calculation using the upper limit for the $P_{11}(1440)$ coupling to the s-wave $\pi\pi$ channel, can be excluded. In the future, the present data might be exploited to provide a better constraint on this coupling. Additionally, the cross section is compared to the calculation with the chiral unitary model [20], which especially at threshold predicts a

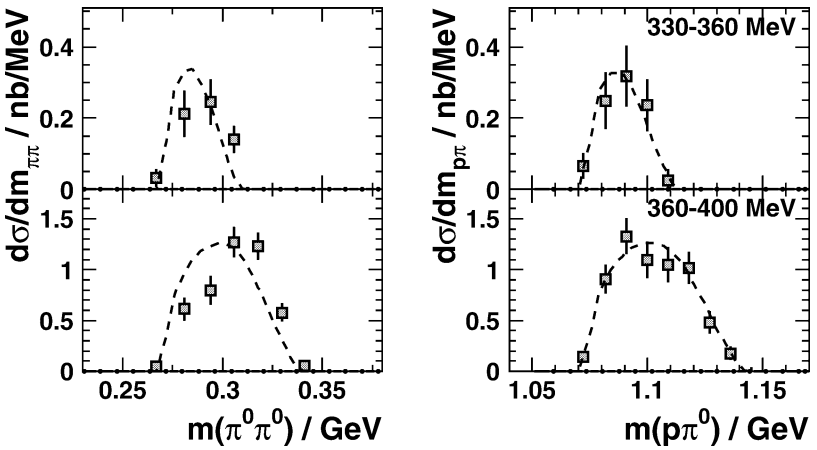

Fig. 3. Invariant mass of $\pi^0\pi^0$ and $\pi^0 p$ for different bins of beam energy (full squares). The dashed curve shows 3 body phase space. The beam energy range in the upper panel is 330–360 MeV and in the lower panel 360–400 MeV.

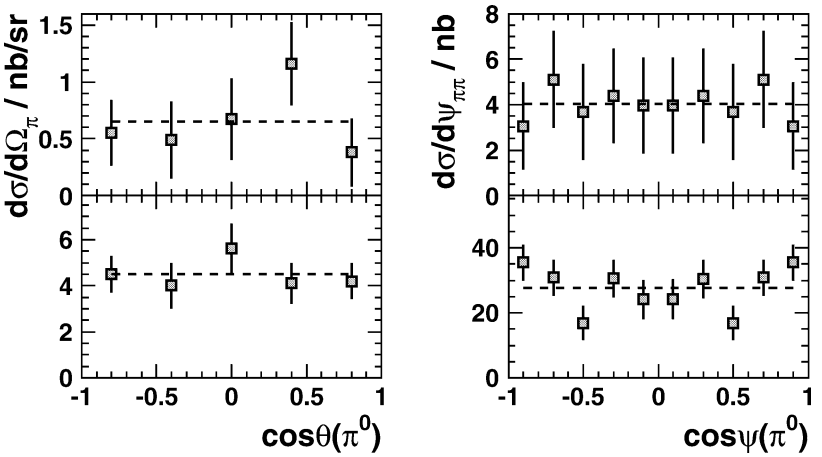

Fig. 4. Angular distributions of the center of mass polar angle θ_{π^0} (left panel) and the angle ψ_{π^0} (right panel) between the proton and the two-pions in the $\pi^0\pi^0$ rest frame (Gottfried–Jackson system). The dashed curve shows 3 body phase space. The beam energy range in the upper panel is 330–360 MeV and in the lower panel 360–400 MeV.

smaller cross section. The data show good agreement with both calculations.

Fig. 3 shows the invariant masses of the $\pi^0\pi^0$ and $p\pi^0$ systems in the incident energy beam ranges of 330–360 MeV and 360–400 MeV. The $p\pi^0$ mass is consistent with a three body phase space distribution, whereas the $\pi^0\pi^0$ mass deviates slightly already for the energy bin of 330–360 MeV from the phase space distributions and shows a trend towards higher invariant masses. The Valencia chiral unitary model [20] explains that $m_{\pi^0\pi^0}$ distributions skewed to higher invariant masses can arise from the interference of the isospin $I = 0$ and $I = 2\pi^0\pi^0$ amplitudes.

Two angular distributions are depicted in Fig. 4. The polar angle θ_{π^0} of the π^0 mesons in the overall center of mass frame is consistent with an isotropic distribution. The same holds for the angle between the π^0 mesons ψ_{π^0} and the proton in the frame where the $\pi^0\pi^0$ system is at rest (Gottfried–Jackson system). Due to the indistinguishability of the two π^0 mesons, the distribution of ψ_{π^0} shows a symmetry around 90°. The isotropy with respect to the ψ_{π^0} angle in

both energy ranges indicates, that the π^0 mesons are dominantly in an s-wave state.

In summary, we have measured the total cross section at threshold for the reaction $\gamma p \to \pi^0\pi^0 p$. This experiment was motivated as a test of a ChPT calculation [8] which shows an unexpectedly high $2\pi^0$ rate compared to final states including charged pions. This fact is attributed to a dominant contribution of pion loops which appear in leading (nonvanishing) order. This prediction is in agreement with our measured data. Furthermore, the upper limit quoted for this prediction can be excluded. In future it might be possible to exploit the present data to give a better constraint on the $P_{11}(1440)$ to s-wave $\pi\pi$ coupling. Secondly, the data are also compared to a prediction [20], where pion loops are dynamically generated. Especially close to threshold, the two predicted cross sections differ significantly. Although the present data are of much superior statistical quality than previous measurements, the precision is still not good enough to discriminate between these two models. The observed angular distribution show that the π^0 mesons are dominantly emitted in an s-wave state.

Acknowledgements

We thank the accelerator group of MAMI as well as many other scientists and technicians of the Institut für Kernphysik at the University of Mainz for their outstanding support. This work is supported by DFG Schwerpunktprogramm: “Untersuchung der hadronischen Struktur von Nukleonen und Kernen mit elektromagnetischen Sonden”, SFB221, SFB443, the UK Engineering and Physical Sciences Research Council and Schweizerischer Nationalfond.

References

[1] J. Ahrens, et al., Nucl. Phys. News 4 (1994) 5.
[2] I. Anthony, et al., Nucl. Instrum. Methods A 301 (1991) 230.
[3] R. Beck, et al., Phys. Rev. Lett. 65 (1990) 1841.
[4] V. Bernard, et al., Phys. Lett. B 268 (1990) 291.
[5] V. Bernard, et al., Nucl. Phys. B 383 (1992) 442.
[6] V. Bernard, et al., Nucl. Phys. A 580 (1994) 475.
[7] V. Bernard, N. Kaiser, U.G. Meissner, Nucl. Phys. B 457 (1995) 147.
[8] V. Bernard, N. Kaiser, U.G. Meissner, Phys. Lett. B 382 (1996) 19.
[9] R. Brun, et al., GEANT3 Users Guide, CERN, Data Handling Division DD/EE/84-1, 1986.
[10] N. Fettes, U.-G. Meissner, Nucl. Phys. A 676 (2000) 311.
[11] A.R. Gabler, et al., Nucl. Instrum. Methods A 346 (1994) 168.
[12] J. Gasser, H. Leutwyler, Ann. Phys. 158 (1984) 142.
[13] F. Haerter, et al., Phys. Lett. B 401 (1997) 229.
[14] S.J. Hall, et al., Nucl. Instrum. Methods A 368 (1996) 698.
[15] E. Jenkins, A.V. Manohar, Phys. Lett. B 255 (1991) 558.
[16] M. Kotulla, et al., Phys. Rev. Lett. 89 (2002) 272001.
[17] M. Kotulla, Prog. Part. Nucl. Phys. 50 (2) (2003) 295.
[18] E. Mazzucato, et al., Phys. Rev. Lett. 57 (1986) 3144.
[19] R. Novotny, IEEE Trans. Nucl. Sci. 38 (1991) 379.
[20] L. Roca, E. Oset, M.J. Vincente Vacas, Phys. Lett. B 541 (2002) 77.
[21] J.A. Gomez Tejedor, E. Oset, Nucl. Phys. A 600 (1996) 413.
[22] Th. Walcher, Prog. Part. Nucl. Phys. 24 (1990) 189.
[23] S. Weinberg, Physica A 96 (1979) 327.
[24] M. Wolf, et al., Eur. Phys. J. A 9 (2000) 5.